Single versus Double Proton-Transfer Reactions in Watson−Crick Base Pair Radical Cations. A Theoretical Study

Juan Bertran,* Antonio Oliva, Luis Rodríguez-Santiago, and Mariona Sodupe

Contribution from the Departament de Química, Universitat Autònoma de Barcelona, Bellaterra, 08193 Spain

Received February 9, 1998. Revised Manuscript Received May 18, 1998

Abstract: Single and double proton-transfer reactions in Watson−Crick Guanine−Cytosine (GC) and Adenine−Thymine (AT) radical cations have been studied using the hybrid density functional B3LYP method. Calibration calculations for the formamidine−formamide dimer, a model system of AT, have shown that B3LYP compares well to the high level ab initio correlated method CCSD(T), both for the neutral and cationic systems. The single proton-transfer reaction is favorable in both the GC and AT radical cations; it takes place from the ionized monomer (guanine and adenine, respectively), which increases its acidity, to the neutral fragment. For the two systems, GC and AT, the nonproton transferred and single proton transferred structures are almost degenerate ($\Delta E = 1.2$ kcal/mol), and the process presents low energy barriers (4.3 kcal/mol for GC and 1.6 kcal/mol for AT). The double proton-transfer reaction is less favorable than the single one, in contrast to what is observed for the neutral systems. The relative stability of the different structures can be understood considering two factors: the relative stability of the asymptotes from which they derive and the number and sequence of the strong and weak hydrogen bonds formed. For the same number of strong short hydrogen bonds, the most stable structures are those in which the strong H-bonds are neighbors. Based on these considerations, a prediction for other pairings is reported.

1. Introduction

One-electron oxidations in DNA have recently received considerable attention due to their connection with DNA damage caused by ionizing radiation,[1] oxidizing agents,[2] and photoirradation using endogenous photosensitizers.[3] The initial ionization of DNA by the 193-nm light is predicted to occur mainly at the guanine residue, which has the lowest ionization potential.[4] Moreover, initially oxidized radical species on other fragments can migrate to the most easily oxidized nucleobase guanine. Thus, the DNA damage is predicted to be produced at this site.[1e,5]

One proposed pathway[1e] to strand breakage in DNA goes through deprotonated species of the guanine radical cation that produce specific hydrogen atom abstraction reactions from the sugar moiety, causing the heterolytic elimination of the phosphate ester bond.[6] Moreover, proton-transfer reactions between base pair ion radicals or to surrounding hydrogen bonded water molecules can be important determinants of ion radical stabilization and migration in DNA.[2d,7] So, it is not surprising that single proton-transfer reactions between base pair radical cations have been studied from a theoretical point of view. In particular, the pioneering work of Sevilla and co-workers[8] and the more recent work of Clark and co-workers[9] must be mentioned.

The double proton-transfer reaction in DNA base pairs has been hypothesized as a possible source of spontaneous muta-

(1) (a) Sevilla, M. D.; Becker, D.; Yan, M.; Summerfield, S. R *J. Phys. Chem.* **1991**, *95*, 3410. (b) Yan, M.; Becker, D.; Summerfield, S. R.; Renke, P.; Sevilla, M. D. *J. Phys. Chem.* **1992**, *96*, 1983. (c) Melvin, T.; Plumb, M. A.; Botchway, S. W.; O'Neill, P.; Parker, A. W. *Photochem. Photobiol.* **1995**, *61*, 584. (d) Cullis, P. M.; Malone, M. E.; Merson-Davies, L. A. *J. Am. Chem. Soc.* **1996**, *118*, 2775. (e) Melvin, T.; Botchway, S. W.; Parker, A. W.; O'Neill, P. O. *J. Am. Chem. Soc.* **1996**, *118*, 10031. (f) deLara, C. M.; Jenner, T. J.; Townsend, K. M. S.; Marsden, S. J.; O'Neill, P. *Radiat. Res.* **1995**, *144*, 43. (g) O'Neill, P.; Fielden, E. M. *Adv. Radiat. Biol.* **1993**, *17*, 53. (h) Görner, H. *J. Photochem. Photobiol. B* **1994**, *26*, 117. (i) Candeias, L. P.; O'Neill, P.; Jones, G. D. D.; Steenken, S. *Int. J. Radiat. Biol.* **1992**, *61*, 15. (j) Angelov, D.; Spassky, A.; Berger, M.; Cadet, J. *J. Am. Chem. Soc.* **1997**, *119*, 11373.

(2) (a) Johnston, D. H.; Glasgow, K. C.; Thorp, H. H. *J. Am. Chem. Soc.* **1995**, *117*, 8933. (b) O'Neill, P.; Fielden, E. M. *Adv. Radiat. Biol.* **1993**, *17*, 53. (c) O'Neill, P.; Davies, S. E. *Int. J. Radiat. Biol.* **1987**, *52*, 577. (d) Steenken, S. *Chem. Rev.* **1989**, *89*, 503. (e) Breen, A. P.; Murphy, J. A. *Free Radical Biol. Med.* **1995**, *18*, 1033. (f) Simic, M. G. *Cancer Res.* **1993**, *53*, 2. (g) Candeias, L. P.; Steenken, S. *J. Am. Chem. Soc.* **1992**, *114*, 699.

(3) (a) Stemp, E. D. A.; Arkin, M. R.; Barton, J. K. *J. Am. Chem. Soc.* **1997**, *119*, 2921. (b) Hall, D. B.; Holmlin, R. E.; Barton, J. K. *Nature* **1996**, *382*, 731. (c) Murphy, C. J.; Arkin, M. R.; Ghatlia, N. D.; Bossmann, S.; Turro, N. J.; Barton, J. K. *Proc. Nat. Acad. Sci. U.S.A.* **1994**, *91*, 5315. (d) Arkin, M. R.; Stemp, E. D. A.; Turro, C.; Turro, N. J.; Barton, J. K. *J. Am. Chem. Soc.* **1996**, *118*, 2267. (e) Holmlin, R. E.; Stemp, E. D. A.; Barton, J. K. *J. Am. Chem. Soc.* **1996**, *118*, 5236. (f) Arkin, M. R.; Stemp, E. D. A.; Holmlin, R. E.; Barton, J. K.; Hörmann, A.; Olson, E. J. C.; Barbara, P. F. *Science* **1996**, *273*, 475. (g) Saito, I.; Takayama, M.; Sugiyama, H.; Nakatani, K.; Tsuchida, A.; Yamamoto, M. *J. Am. Chem. Soc.* **1995**, *117*, 6406. (h) Saito, I.; Takayama, M.; Kawanishi, S. *J. Am. Chem. Soc.* **1995**, *117*, 5590. (i) Breslin, D. T.; Schuster, G. B. *J. Am. Chem. Soc.* **1996**, *118*, 2311. (j) Ito, K.; Inone; S.; Yamamoto, K.; Kawanishi, S. *J. Biol. Chem.* **1993**, *268*, 13221. (k) Ly, D.; Kan, Y.; Armitage, B.; Schuster, G. B. *J. Am. Chem. Soc.* **1996**, *118*, 8747.

(4) (a) Colson, A. O.; Besler, B.; Sevilla, M. D. *J. Phys. Chem.* **1993**, *97*, 8092. (b) Sevilla, M. D.; Besler, B.; Colson, A. O. *J. Phys. Chem.* **1995**, *99*, 1060.

(5) Melvin, T.; Botchway, S.; Parker, A. W.; O'Neill, P. *J. Chem. Soc. Chem. Commun.* **1995**, 653.

(6) (a) Breen, A. P.; Murphy, J. A. *Free Radical Biol. Med.* **1995**, *18*, 1033. (b) Giese, B.; Beyrich-Graf, X.; Erdmann, P.; Giraud, L.; Imwinkelried, P.; Muller, S. N.; Schwitter, U. *J. Am. Chem. Soc.* **1995**, *117*, 6146. (c) Giese, B.; Beyrich-Graf, X.; Erdmann, P.; Petretta, M.; Scwitter, U. *Chem. Biol.* **1995**, *2*, 367. (d) Gugger, A.; Batra, R.; Rzadek, P.; Rist, G.; Giese, B. *J. Am. Chem. Soc.* **1997**, *119*, 8740.

(7) (a) Steenken, S.; Telo, J. P.; Novais, H. M.; Caudeias, L. P. *J. Am. Chem. Soc.* **1992**, *114*, 4701. (b) Steenken, S. *Free Radical Res. Comm.* **1992**, *16*, 349. (c) Symons, M. C. R. In The early Effects of Radiation on DNA. Fielden, E. M., O'Neill, P., Eds.; Springer-Verlag: Berlin, 1991; pp 111−124.

S0002-7863(98)00441-7 CCC: $15.00
Published on Web 07/31/1998

tions,[10] since rare tautomers could be formed which might disturb the genetic code. Theoretical studies on double proton-transfer processes have been considered for the ground state of neutral pairs. Because of the size of the Adenine−Thymine (AT) and Guanine−Cytosine (GC) base pairs, however, lower computational levels of theory have been used till recently. First studies, using ab initio[11] and semiempirical methods[12] were performed using fixed geometries for the monomers during the proton-transfer processes. Consequently, both the single and double proton-transfer reactions were found to be too unfavorable. Recent studies,[13] in which full geometry optimizations have been performed, have found smaller reaction energies. Nevertheless, all studies agree with the fact that the single proton-transfer reaction is less favorable than the double proton-transfer one, because the single transfer process implies a charge separation in the formation of the resulting ion−pair complex, while in the double proton-transfer process the electroneutrality is maintained. The energy barrier in double proton-transfer processes is always high,[13c] regardless of whether the mechanism is concerted or two-step.

Recent experimental[14] and theoretical studies[15] on radical cations have shown that the interconversion between different isomeric species can be catalyzed by polar neutral molecules, such as water, in what Bohme[16] has termed proton-transport catalyst. This catalysis implies a double proton-transfer process. Ionization of the AT and GC base pairs is expected to be localized in the monomers with the lowest ionization potentials: Adenine and Guanine, respectively.[4] Thymine and Cytosine could then play the role of the neutral molecule in the proton-transport catalyst, and so, the double proton-transfer process is expected to be kinetically more favorable in this case than in the neutral base pair.

Molecular beam experiments have allowed the study of base-pairing in gas phase,[17] the ionization potentials of hydrated Adenine and Thymine,[18] and double proton-transfer processes in model base pairs in excited states.[19] In consequence, theoretical studies on base pair systems can, nowadays, be tested experimentally, which makes theory and experiment complementary tools in order to get a deeper insight in chemical and biochemical processes.

In this work we present a theoretical study of the ionized Watson−Crick base pairs. Energies, geometries, and vibrational frequencies have been determined using theoretical methods that include electron correlation. Our main goal is to understand the behavior of the base pair after ionization, focusing on the difference between single and double proton-transfer reactions. We expect that the present work will provide some insight and help understand the complex processes of the DNA damage, caused by ionization radiation or oxidizing agents.

2. Methods

Full geometry optimizations and frequency calculations for the neutral and cationic base pairs have been performed using the hybrid three-parameter B3LYP density functional method[20] with the 6-31G** basis set.[21] The adequacy of density functional methods for the study of hydrogen bonded compounds has been the subject of several recent papers.[22] These studies have shown that the nonlocal methods that include gradient corrections, in particular the B3LYP one, provide results comparable to MP2 when similar basis sets are used. Moreover, for different radical cations, the B3LYP method has been shown to perform much better than the more computationally demanding UMP2 one,[23] due to the fact that the perturbation expansion converges slowly when the UHF reference wave function has large spin contamination.[24] In contrast, B3LYP does not overestimate spin polarization, which has been related to spin contamination.[25]

Since it is desirable to confirm the B3LYP results for this kind of systems, we have performed calculations for a model system using ab initio highly correlated methods and larger basis sets. The model system chosen is the formamidine−formamide complex which has two hydrogen bonds similar to those found in the adenine−thymine base pair.[26] For this model system, geometry optimizations have been carried out at the B3LYP and MP2 levels of calculations using the same 6-31G** basis set. All geometry optimizations have been performed using C_s

(8) (a) Colson, A. O.; Besler, B.; Sevilla, M. D. *J. Phys. Chem.* **1992**, *96*, 9787. (b) Colson, A. O.; Sevilla, M. D. *Int. J. Radiat. Biol.* **1995**, *67*, 627.

(9) Hutter, M.; Clark, T. *J. Am. Chem. Soc.* **1996**, *118*, 7574.

(10) (a) Löwdin, P. O. *Rev. Mod. Phys.* **1963**, *35*, 724. (b) Löwdin, P. O. *Adv. Quantum Chem.* **1965**, *2*, 213.

(11) (a) Clementi, E.; Mehl, J.; von Niessen, W. *J. Chem. Phys.* **1971**, *54*, 508. (b) Clementi, E. *Proc. Natl. Acad. Sci. U.S.A.* **1972**, *69*, 2942. (c) Kong, Y. S.; John, M. S.; Löwdin, P. O. *Int. J. Quantum Chem. Quantum Biol. Symp.* **1987**, *14*, 189.

(12) (a) Rein, R.; Harris, F. E. *J. Chem. Phys.* **1964**, *41*, 3393. (b) Lunell, S.; Sperber, G. *J. Chem. Phys.* **1967**, *46*, 2119. (c) Scheiner, S.; Kern, C. W. *J. Am. Chem. Soc.* **1979**, *101*, 4081. (d) Scheiner, S.; Kern, C. W. *Chem. Phys. Lett.* **1978**, *57*, 331.

(13) (a) Hrouda, V.; Florián, J.; Hobza, P. *J. Phys. Chem.* **1993**, *97*, 1542. (b) Florián, J.; Hrouda, V.; Hobza, P. *J. Am. Chem. Soc.* **1994**, *116*, 1457. (c) Florián, J.; Leszczynski, J. *J. Am. Chem. Soc.* **1996**, *118*, 3010.

(14) (a) Audier, H. E.; Leblanc, D.; Mourgues, P.; McMahon, T. M.; Hammerum, S. *J. Chem. Soc., Chem Commun.* **1994**, 2329. (b) Mourgues, P.; Audier, H. E.; Leblanc, D.; Hammerum, S. *Org. Mass Spectrom.* **1993**, *28*, 1098. (c) Audier, H. E.; Fossey, J.; Mourgues, P. *J. Phys. Chem.* **1996**, *100*, 18380.

(15) (a) Gauld, J. W.; Audier, H. E.; Fossey, J.; Radom, L. *J. Am. Chem. Soc.* **1996**, *118*, 6299. (b) Chalk, A. J.; Radom, L. *J. Am. Chem. Soc.* **1997**, *119*, 7573. (c) Gauld, J. W.; Radom, L. *J. Am. Chem. Soc.* **1997**, *119*, 9831. (d) Coitiño, E. L.; Lledós, A.; Serra, A.; Bertran, J.; Ventura, O. N. *J. Am. Chem. Soc.* **1993**, *115*, 9121.

(16) Bohme, D. K. *Int. J. Mass Spectrom. Ion Proc.* **1992**, *115*, 95.

(17) Dey, M.; Moritz, F.; Grotemeyer, J.; Schlag, E. W. *J. Am. Chem. Soc.* **1994**, *116*, 9211.

(18) Kim, S. K.; Lee, W.; Herschbach, D. R. *J. Phys. Chem.* **1996**, *100*, 7933.

(19) (a) Douhal. A.; Kim, S. K.; Zewail, A. H. *Nature* **1995**, *378*, 260. (b) Lopez-Martens, R.; Long, P.; Solgadi, D.; Soep, B.; Syage, J.; Millie, Ph. *Chem. Phys. Lett.* **1997**, *273*, 219.

(20) (a) Becke, A. D. *J. Chem. Phys.* **1993**, *98*, 5648. (b) Lee, C.; Yang, W.; Parr, R. G. *Phys. Rev. B* **1988**, *37*, 785. (c) Stevens, P. J.; Devlin, F. J.; Chablowski, C. F.; Frisch, M. J. *J. Phys. Chem.* **1994**, *98*, 11623.

(21) Hariharan, P. C.; Pople, J. A. *Theor. Chim. Acta* **1973**, *28*, 213.

(22) (a) Novoa, J. J.; Sosa, C. *J. Phys. Chem.* **1995**, *99*, 15837. (b) Lee, C.; Fitzgerald, G.; Planas, M.; Novoa, J. J. *J. Phys. Chem.* **1996**, *100*, 7398. (c) Lee, C.; Sosa, C.; Planas, M.; Novoa, J. J. *J. Chem. Phys.* **1996**, *104*, 7081. (d) Sim, F.; St-Amant, A.; Papai, I.; Salahub, D. R. *J. Am. Chem. Soc.* **1992**, *114*, 4391. (e) Wei, D.; Salahub, D. R. *J. Chem. Phys.* **1994**, *101*, 7633. (f) Del Bene, J. E.; Person, W. B.; Szczepaniak, K. *J. Phys. Chem.* **1995**, *99*, 10705. (g) Kieninger, M.; Suhai, S. *Int. J. Quantum Chem.* **1994**, *52*, 465. (h) Gonzalez, L.; Mo, O., Yañez, M.; Elguero, J. *J. Mol. Struct. Theochem.* **1996**, *371*, 1. (i) Latajka, Z.; Bouteiller, Y.; Scheiner, S. *Chem. Phys, Lett.* **1995**, *234*, 159. (j) Latajka, Z.; Bouteiller, Y. *J. Chem. Phys.* **1994**, *101*, 9793. (k) Kim, K.; Jordan, K. D. *J. Phys. Chem.* **1994**, *98*, 10089. (l) Alfredsson, M.; Ojanäe, L.; Hermansson, K. G. *Int. J. Quantum Chem.* **1996**, *60*, 767. (m) Florián, J.; Johnson, B. G. *J. Phys. Chem.* **1995**, *99*, 5899. (n) Combarida, J. E.; Kestner, N. R. *J. Phys. Chem.* **1995**, *95*, 2717.

(23) (a) Ventura, O. N.; Kieninger, M.; Coitiño, E. L. *J. Comput. Chem.* **1996**, *17*, 1309. (b) Barone, V.; Adamo, C. *Chem. Phys. Lett.* **1994**, *224*, 432. (c) Barone, V. *Theor. Chim. Acta* **1995**, *91*, 113. (d) Znilhof, H.; Dinnocenzo, J. P.; Chandrasekhar, A.; Shaik, S. *J. Phys. Chem.* **1996**, *100*, 15774. (e) Baker, J.; Muir, M.; Andzelm, J. *J. Chem. Phys.* **1995**, *102*, 2063. (f) Sodupe, M.; Oliva, A.; Bertran, J. *J. Phys. Chem. A* **1997**, *101*, 9142.

(24) (a) Handy, N. C.; Knowles, P. J.; Somasundran, K. *Theor. Chim. Acta* **1985**, *68*, 87. (b) Tozer, D. J.; Handy, N. C.; Amos, R. D.; Pople J. A.; Nobes, R. H.; Yaoming, X.; Schaefer, H. F. *Mol. Phys.* **1993**, *79*, 777.

(25) (a) Baker, J.; Scheiner, A.; Andzelm, J. *Chem. Phys. Lett.* **1993**, *216*, 380. (b) Barone, V.; Adamo, C. *Chem. Phys. Lett.* **1994**, *224*, 432.

(26) Sponer, J.; Hobza, P. *Chem. Phys.* **1996**, *204*, 365.

Table 1. Relative Energies[a] of the Neutral and Cationic FI−FA Dimers, with Respect to FI + FA and FI^+ ($^2A''$) + FA Asymptotes, Respectively[b]

		cationic			
	neutral FI−FA	$FI^{\bullet+}$−FA	$FI^{\bullet}(-H^+)-FA(+H^+)$	$FI^{\bullet}(-H^+) + FA(+H^+)$	$FI^{\bullet+} + FA'$
B3LYP//B3LYP	−17.8(−14.3)		−34.5(−32.8)	+8.7	+12.6
MP2//B3LYP	−17.3(−12.6)		−30.3(−28.3)	+13.0	+12.3
PMP2//B3LYP			−33.3	+10.1	
CCSD(T)//B3LYP	−16.8		−34.1	+7.8	+10.9
CCSD(T)//B3LYP cc-VTZ	−15.7		−33.6	+6.0	+9.9
MP2//MP2	−17.4	−28.0	−29.7	+13.6	+12.3
PMP2//MP2		−30.6	−33.8	+9.5	
CCSD(T)//MP2	−17.0	−30.3	−34.3	+7.6	+10.9

[a] In kcal/mol. Calculations performed using C_s symmetry. [b] In parentheses counterpoise corrected energies.

symmetry. For the ($^2A''$) cationic dimer, the planar structures are found to be minima both at the B3LYP and MP2 levels of calculations. For the neutral dimer and free monomers some structures are found to be first order saddle points, depending on the level of calculation. Since our purpose is to compare different levels of theory, we report only the calculations obtained using C_s symmetry. Single point calculations, both at the B3LYP and MP2 equilibrium geometries, have been performed using the CCSD(T) method.[27] The effect of increasing the basis set is studied at the CCSD(T) level at the B3LYP equilibrium geometries. The larger basis are the correlation consistent sets of Dunning.[28] For C, N, and O we have used the (10s5p2d)/[4s3p2d] set and for H the (5s2p)/[3s2p]. For the MP2 and CCSD(T) calculations, we have correlated all the electrons except the 1s-like ones.

Basis set superposition error has been corrected by using the counterpoise correction.[29] Calculations with the small basis set are based on a spin unrestricted formalism and have been performed with the Gaussian94 package.[30] CCSD(T) calculations with the larger basis set are spin restricted and have been done with the MOLPRO 96 package.[31]

3. Model System: Formamidine−Formamide Dimer

Formamidine (FI) and formamide (FA) molecules interact forming two parallel hydrogen bonds. Figure 1 shows the B3LYP and MP2 optimized geometries of the neutral (FI−FA) and cationic $(FI-FA)^+$ dimers. The interaction energies with respect to the ground-state asymptotes are presented in Table 1.

The ionization of the dimer takes place at the formamidine fragment, since it is the monomer with lower ionization potential. The formamidine monomer becomes then more acid, and so, the proton-transfer reaction to formamide can occur easily. A second proton-transfer reaction from the protonated formamide, $FA(+H^+)$, to the deprotonated formamidine $FI^{\bullet}(-H^+)$ monomer could also take place. The following scheme show the two processes:

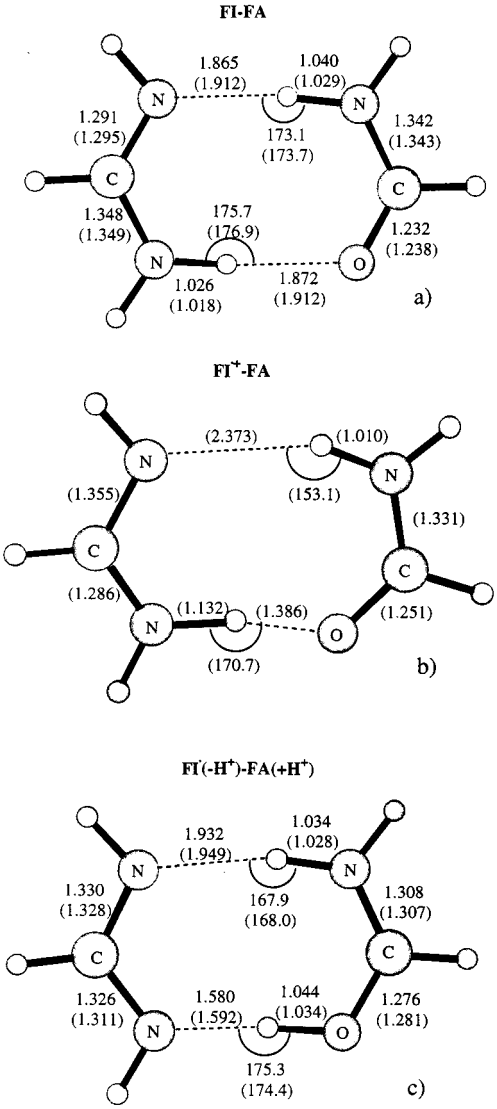

Figure 1. B3LYP (MP2) optimized geometrical parameters of the neutral (a) and cationic (b and c) formamidine−formamide dimers. Distances are in Å and angles in deg.

Let us first consider the neutral system. It can be observed in Figure 1 that B3LYP and MP2 methods provide similar geometries. The largest differences correspond to the H-bond distances, which are about 0.04−0.05 Å smaller at the B3LYP level. Previous studies on neutral hydrogen bonded systems[22] found that B3LYP tends to provide somewhat smaller H-bond

(27) Raghavachari, K.; Trucks, G. W.; Pople, J. A.; Head-Gordon, M. *Chem. Phys. Lett.* **1989**, *57*, 479.
(28) Dunning, T. H. *J. Chem. Phys.* **1989**, *90*, 1007.
(29) Boys, S. F.; Bernardi, F. *Mol. Phys.* **1970**, *19*, 553.
(30) Frisch, M. J.; Trucks, G. W.; Schlegel, H. B.; Gill, P. M. W.; Johnson, B. G.; Robb, M. A.; Cheesman, J. R.; Keith, T. A.; Petersson, G. A.; Montgomery, J. A.; Raghavachari, K.; Al-Laham, M. A.; Zakrzewsky, V. G.; Ortiz, J. V.; Foresman, J. B.; Cioslowsky, J.; Stefanov, B.; Nanayakkara, A.; Challacombe, M.; Peng, C. Y.; Ayala, P. Y.; Chen, W.; Wong, M. W.; Andrés, J. L.; Replogle, E. S.; Gomperts, R.; Martin, R. L.; Fox, D. J.; Binkley, J. S.; Defrees, D. J.; Baker, J.; Stewart, J. J. P.; Head-Gordon, M.; Gonzalez, C.; Pople, J. A. Gaussian 94, Revision D.1; Gaussian Inc.: Pittsburgh, PA, 1995.
(31) MOLPRO is a package of ab initio programs written by H.-J. Werner and P. J. Knowles, with contributions from J. Almlöf, R. D. Amos, A. Berning, M. J. O. Deegan, F. Eckert, S. T. Elbert, C. Hampel, R. Lindh, W. Meyer, A. Nicklass, K. Peterson, R. Pitzer, A. J. Stone, P. R. Taylor, M. E. Mura, P. Pulay, M. Schuetz, H. Stoll, T. Thorsteinsson, and D. L. Cooper. The CCSD program is described: Hampel, C.; Peterson, K.; Werner, H.-J. *Chem. Phys. Lett.* **1992**, *190*, 1.

Scheme 1

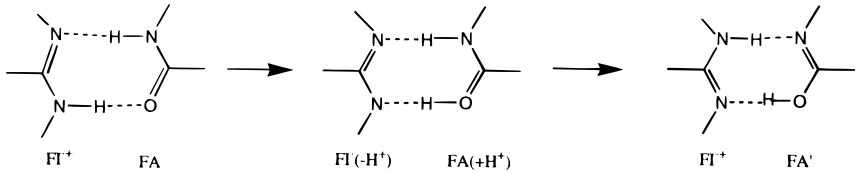

distances and smaller dimerization energies than MP2. The smaller interaction energies have been attributed to the fact that the dispersion energy is not covered by present density functional methods.[32] In the present system (FI−FA), we observe the same tendency for the H-bond distances, but the interaction energy at the B3LYP level is slightly larger than the one obtained with correlated ab initio methods. The difference between MP2 and B3LYP dimerization energies increases after including the counterpoise correction. Table 1 shows that the effect of the geometry in the dimerization energy is very small; that is, if a consistent set of geometries is used, the binding energy differs by less than 0.2 kcal/mol whether we use the equilibrium MP2 or B3LYP geometries. Thus, the differences between B3LYP and conventional ab initio methods arise mainly from the electrostatic term, which varies due to the different procedure of including electron correlation, the dispersion effects being a minor component of the total interaction energy. Overall, the B3LYP value is in good agreement with the MP2 and CCSD(T) ones. Similar results have been observed previously for the formamide−formamide dimer.[33] At the highest level of calculation, CCSD(T), the increase of the basis set decreases the binding energy by 1.1 kcal/mol due to the smaller basis set superposition error. The obtained value differs only by 1.4 kcal/mol from the counterpoise corrected B3LYP obtained with the smaller basis set.

For the cationic system, we have investigated the three isomers shown in Scheme 1, at the B3LYP and MP2 levels of theory. A minimum corresponding to the single proton transferred isomer, FI$^{\bullet}(-H^+)-FA(+H^+)$, has been localized at both levels of calculation. However, the nonproton transferred FI$^{\bullet+}$−FA complex has only been determined at the MP2 level. B3LYP calculations always collapsed to the single proton transferred complex. As it was found for the phenol-ammonia cation,[23f] the nonproton transferred minimum at the MP2 level is probably an artifact produced by the spin contamination of the reference wave function ($S^2 = 1.0$). Note that the projected MP2 energies as well as the values obtained with the more extensive electron correlation CCSD(T) method increase the stability of the FI$^{\bullet}(-H^+)-FA(+H^+)$ isomer compared to that of FI$^{\bullet+}$−FA. It is worth noting that B3LYP values compare much better to the more reliable CCSD(T) and projected MP2 results than to the unprojected ones. Increasing the basis set decreases slightly the interaction energy at the CCSD(T). Thus, as shown in previous studies,[23] B3LYP seems to perform much better than UMP2 for radical cation systems. As found for the model system, the B3LYP calculations for the base pair radical cations present values of S^2 between 0.76 and 0.78, while the UHF values lie within 0.92 and 1.3.

The double proton transferred FI$^{\bullet+}$−FA′ isomer has not been localized as a minimum on the potential energy surface at any of the two levels. In all cases, geometry optimizations lead to the single proton transferred isomer. As it will be discussed below, the stability of the different isomers can be related to the relative energy of the different asymptotes involved in the dimerization process and to the strength of the hydrogen bonds formed.

In summary, the results obtained for this model system indicate that B3LYP is an appropriate method for studying the Watson−Crick base pairs, both the neutral and cationic systems. Moreover, the lower computational cost of B3LYP compared to other correlated methods allows us to calculate the harmonic vibrational frequencies of these large systems, which are needed for computing thermochemical properties.

4. Watson−Crick Base Pairs

In this section we will present and discuss the results obtained for the neutral and ionized Guanine−Cytosine (GC) and Adenine−Thymine (AT) Watson−Crick base pairs. We will first present the molecular structure, the interaction energies of the two dimers, and the adiabatic ionization potentials. Finally, we will analyze the proton-transfer processes in the radical cations. The results obtained will be compared with those obtained for the neutral base pairs.

4.1. Equilibrium Geometries, Dimerization Energies, and Ionization Potentials. Figure 2 shows the B3LYP/6-31G** equilibrium geometries of the neutral and cationic species of GC and AT base pairs. As shown in previous studies,[34] although the isolated monomers with an NH_2 group are nonplanar, the Watson−Crick GC and AT dimers have C_s symmetry and are planar due to the formation of the hydrogen bonds. The lowest out-of-plane frequencies are, however, very small, which indicates that those dimers are very flexible.

The hydrogen bond distances of the neutral and cationic GC and AT dimers are given in Table 2. For comparison, we have also included the results obtained previously at the Hartree−Fock level[9,35] and the known experimental values.[37] It can be observed that, in all cases, the B3LYP method provides shorter hydrogen bond distances than the Hartree−Fock one, due to the inclusion of electron correlation effects at the B3LYP level. Similar variations have been observed using the traditional correlated MP2 method.[38] At present, the only base pair that has been optimized at the MP2 level is the Cytosine−Cytosine dimer.[36] For this system, the MP2 and B3LYP H-bond lengths are shown to be very similar, and thus, we expect our B3LYP

(32) (a) Kristyán, S.; Pulay, P. *Chem. Phys. Lett.* **1994**, *229*, 175. (b) Hobza, P.; Sponer, J.; Reschel, T. *J. Comput. Chem.* **1995**, *16*, 1315.

(33) (a) Kim, Y. *J. Am. Chem. Soc.* **1996**, *118*, 1522. (b) Lim, J. H.; Lee, E. K.; Kim, Y. *J. Phys. Chem. A* **1997**, *101*, 2233.

(34) (a) Riggs, N. V. *Chem. Phys. Lett.* **1991**, *117*, 447. (b) Gould, I. R.; Hillier, I. H. *Chem. Phys. Lett.* **1992**, *161*, 185. (c) Sponer, J.; Hobza, P. *J. Am. Chem. Soc.* **1994**, *116*, 709. (d) Sponer, J.; Hobza, P. *J. Phys. Chem.* **1994**, *98*, 3161. (e) Sponer, J.; Hobza, P. *J. Mol. Struct. Theochem* **1994**, *304*, 35. (f) Estrin, D. A.; Paglieri, L.; Corongiu, C. *J. Phys. Chem.* **1994**, *98*, 5653. (g) Florián, J.; Leszczynski, J. *J. Biomol. Struct. Dyn.* **1995**, *12*, 1055. (h) Florián, J.; Leszczynski, J. *J. Am. Chem. Soc.* **1996**, *118*, 3010. (i) Sponer, J.; Florián, J.; Hobza, P.; Leszczynski, J. *J. Biomol. Struct. Dyn.* **1996**, *13*, 827. (j) Sponer, J.; Leszczynski, J.; Hobza, P. *J. Phys. Chem.* **1996**, *100*, 5590. (k) Sponer, J. Hobza, P. *Int. J. Quantum Chem.* **1996**, *57*, 959.

(35) Gould, I. R.; Kollman, P. A. *J. Am. Chem. Soc.* **1994**, *116*, 2493.

(36) Sponer, J.; Leszczynski, J.; Hobza, P. *J. Phys. Chem.* **1996**, *100*, 1965.

(37) Saenger, W. Principles of Nucleic Acid Structure; Springer-Verlag: New York; 1984; pp 123 and 124 and references within.

(38) See, for instance: Smallwood, C. J.; McAllister, M. A. *J. Am. Chem. Soc.* **1997**, *119*, 11277.

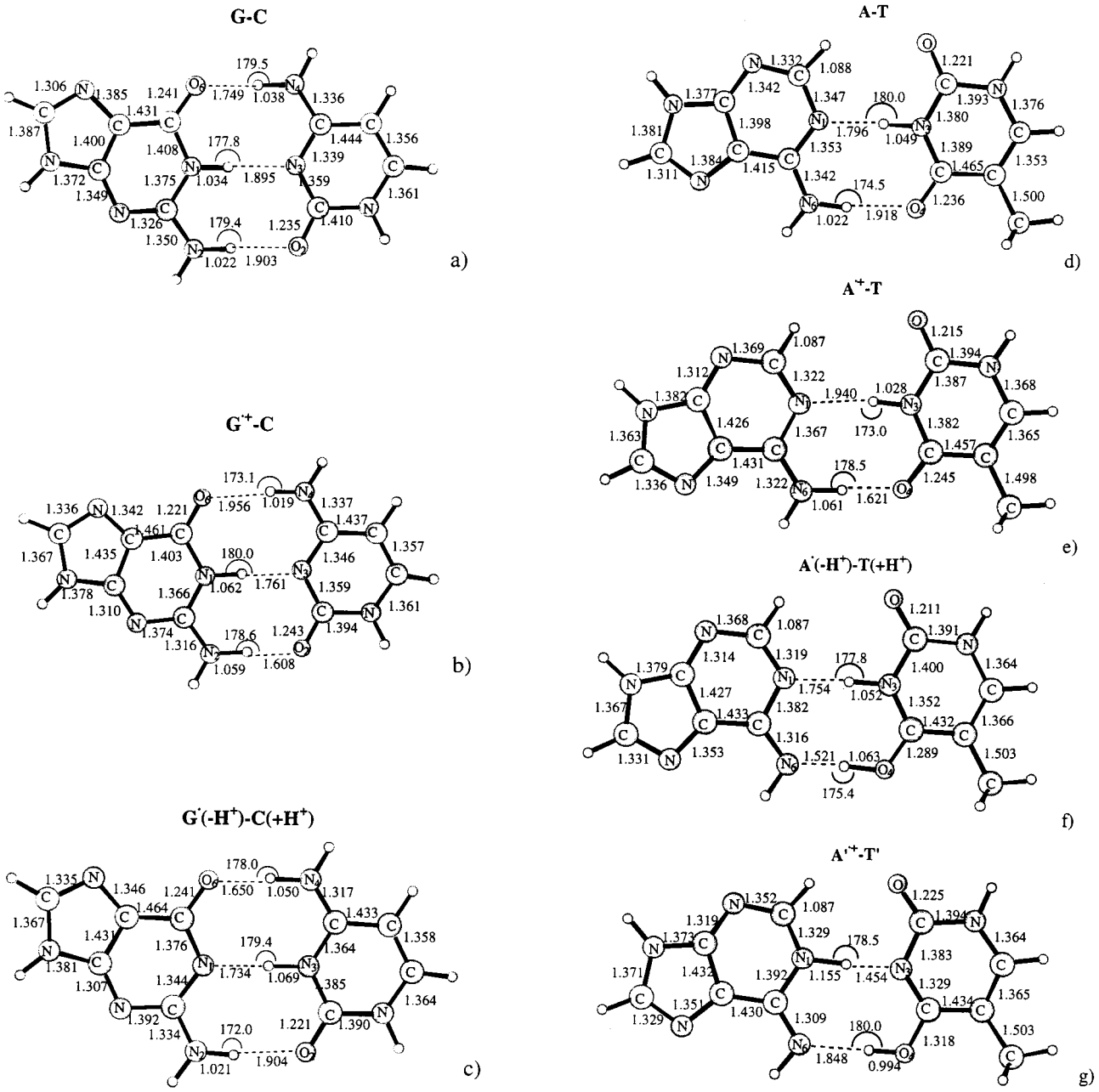

Figure 2. B3LYP optimized geometrical parameters of the neutral and cationic Guanine−Cytosine (a−c) and Adenine−Thymine (d−g) Watson−Crick base pairs. Distances are in Å and angles in deg.

results for GC and AT dimers to be much better than those published up to now at the Hartree−Fock level. This is confirmed by comparison with the experimental values. It can be observed, however, that while the agreement between B3LYP and experiment is very good for AT, the results obtained for GC show larger differences. In particular, the theoretical results show that the O6−N4 distance is shorter than the N2−O2 one, in contrast to the experimental values.[37] Part of this difference may arise from the fact that the experimental results have been obtained from crystallographic data and not from gas-phase studies.

Mulliken charges and spin densities indicate that the ionization of GC and AT is mainly localized at the guanine and adenine monomers, respectively. For GC, the Mulliken charge on guanine is 0.82 and the spin density is 1.00, while for AT, the charge on adenine is 0.79 and the spin density is 0.86. This is not surprising considering that Guanine and Adenine have a lower ionization potential than Cytosine and Thymine, respectively.[4] As for the neutral dimers, the ionized systems have C_s symmetry, the electronic ground-state being a $^2A''$.

Since Guanine and Adenine are the two monomers that loose the electron and thus, become more acid, those hydrogen bonds in which these two monomers act as the proton donor become stronger in the ionized system. This implies a shortening of the distance between the two heavy atoms and a lengthening of the H−X bond involved. In contrast, those H-bonds in which Guanine and Adenine act as the acceptor become weaker. These changes can be observed in Figure 2 and Table 2. That is, the N1−N3 and N2−O2 H-bond distances of GC decrease after ionization while the O6−N4 increases. For AT, the N6−O4 is the bond that gets shorter while the N1−N3 becomes longer.

The interaction energies of neutral and cationic GC and AT dimers are given in Table 3. Correcting for basis set superposition error decreases the B3LYP/6-31G** binding energy by 3−5 kcal/mol. The counterpoise corrected $-\Delta H^0_f$ for neutral GC, obtained including the translational, rotational, and vibrational

Table 2. Hydrogen Bond Distances (Å)

H−bond	HF/6-31G*	HF/6-31G** [c]	B3LYP/6-31G**	exptl[e]
		GC Watson−Crick		
O6···N4	2.93[a,b]	2.92	2.79[c,d]	2.91
N1···N3	3.05[a,b]	3.04	2.93[c,d]	2.95
N2···O2	3.01[a,b]	3.02	2.92[c,d]	2.86
		G$^{\bullet+}$C Watson−Crick		
O6···N4	3.17[b]		2.97[d]	
N1···N3	2.96[b]		2.82[d]	
N2···O2	2.79[b]		2.67[d]	
		AT Watson−Crick		
N1···N3	3.01[a,b]	2.99	2.84[d]	2.82
N6···O4	3.08[a,b]	3.09	2.94[d]	2.95
		A$^{\bullet+}$T Watson−Crick		
N1···N3	3.23[b]		2.96[d]	
N6···O4	2.72[b]		2.68[d]	

[a] Reference 35. [b] Reference 9. [c] Reference 36. [d] Present work. [e] Reference 37.

Table 3. B3LYP Interaction Energies of Watson−Crick Neutral and Cationic GC and AT Base Pairs (in kcal/mol)[c]

	GC		AT	
	neutral	cation	neutral	cation
D_e	30.3(25.5)	48.4(44.3)	16.4(12.3)	25.4(22.3)
D_0[a]	28.8(24.0)	46.8(42.7)	15.3(11.2)	25.1(22.0)
$-\Delta H^0_f$(298 K)[b]	28.8(24.0)	47.1(43.0)	15.0(10.9)	24.8(21.7)
$-\Delta G^0_f$(298 K)	17.4(12.6)	34.1(30.0)	3.8(−0.3)	13.6(10.5)

[a] Includes zero point energy computed from the unscaled harmonic B3LYP frequencies. [b] After correction for translational, rotational, and vibrational energies determined at the B3LYP level. [c] In parentheses are counterpoise corrected values.

thermic corrections at 298 K, (24.0 kcal/mol) is in reasonable agreement with the reported experimental value of 21.0 kcal/mol obtained from field ionization mass-spectrometry studies.[39] Our results are very similar to the DFT values obtained by Santamaría and co-workers,[40] using a different functional, and somewhat larger than previous results obtained at the MP2 level of calculation. It should be noted, however, that those interaction energies were obtained using the equilibrium Hartree−Fock geometries,[35,36] which have been shown to provide too large H-bond distances. Thus, it is not surprising that the stabilizing electrostatic interaction energy is smaller.

It can be observed in Table 3 that ionization produces a significant increase of the binding energy of GC and AT. For GC, the binding energy increases about 19 kcal/mol and for AT 10 kcal/mol both with and without considering the zero point correction. This increase is not due to an equal strengthening of the three hydrogen bonds of GC or the two hydrogen bonds of AT. As it has already been mentioned, ionization strengthens those hydrogen bonds in which the ionized monomer acts as proton donor and weakens those in which it acts as acceptor. Thus, the N1−N3 and N2−O2 hydrogen bonds of GC and the N6−O4 of AT would become strong hydrogen bonds according to the energetical classification (12−24 kcal/mol) reported in ref 41. Moreover, the optimized H-bond distances of these strong bonds are close to the sum of the van der Waal radii, 2.65 for O−N and 2.75 for N−N, and so could be denoted as short-strong hydrogen bonds (SSHB).[42]

A simple thermodynamical cycle shows that the decrease of the ionization potential of the dimers compared to that of the free monomers is just the increase of the binding energy produced by ionization. That is, the lowering of the adiabatic ionization potential, including the zero point energy and correcting for BSSE, of GC compared to G, is 0.81 eV, and that of AT compared to A is 0.47 eV. We expect the lowering of the IP to be more accurate than the computed IP values. Thus, our best estimate of the adiabatic ionization potential of GC (6.96 eV) and AT (7.79 eV) are obtained by subtracting the computed lowering to the experimental IP values[43] of the monomers G and A, respectively.

4.2. Single and Double Proton-Transfer Reactions. Scheme 2 shows the single and double proton-transfer processes studied in the present work.

As already said, the positively charged monomers have an increased acid character. This implies that those H-bonds in which the charged monomer acts as donor are strengthened, while those in which it acts as acceptor are weakened. This has been indicated with the letters s(strong) and w(weak) in Scheme 2.

For G$^{\bullet+}$−C, we have one weak and two neighbor strong H-bonds; that is, a (w−s−s) situation. Any of the two strong H-bonds could be involved in the first proton-transfer reaction. The transfer from N1 to N3 leads to a (s−s−w) situation with two neighbor strong H-bonds, while the transfer from N2 to O2 produces the alternated (s−w−s) pattern. In the first case, the two strong hydrogen bonds can benefit of the enhanced electrostatic interaction by decreasing simultaneously the N1−N3 and N2−O2 distances, while the N4−O6 distance increases to reduce repulsion. These geometry changes can take place through a relative movement of the two monomers which approaches the terminal N2−O2 bond and separates the other N4−O6 terminal bond. Due to the rigidity of the monomers the central H-bond distance does not decrease as much as the terminal one, the obtained value resulting from the compromise of the two terminal strong and weak H-bond interactions. In the second case, we have an alternated (s−w−s) pattern which is less favorable given that we have a central weak bond, which does not allow to obtain a geometrical compromise that benefit strong short H-bonds, without introducing the central H-bond into a repulsive region. As a matter of fact, this structure has not been located as a stationary point on the potential energy surface. Thus, we have only considered the structures shown in Scheme 2.

It can be observed that the double proton-transfer structure G′$^{\bullet+}$−C′ shows also an alternated (s−w−s) situation. Thus, it is not surprising that any attempt to localize this energy minimum collapsed to the single proton-transfer structure. The optimized H-bond distances (Figure 2b,c) agree with what is expected.

For the A$^{\bullet+}$−T dimer, we have one weak and one strong H-bond (w−s) before any proton transfer is produced. After the single proton-transfer reaction, the positive charge moves to the protonated Thymine, and thus, both H-bonds become strong (s−s). The second proton-transfer reaction leads us to a situation similar to the initial one but with the two H-bonds reversed (s−w). The values of the optimized H-bond distances shown in Figure 2e−g confirm the expected changes. It is worth noting the particularly small H-bond distances of 2.58 Å, obtained for N6−O4 in the single proton transferred structure (Figure 2f), and of 2.61 Å, obtained for N1−N3 in the double proton-transfer one (Figure 2g). These distances are much smaller than the sum of van der Waals radii, typically observed in strong-short hydrogen bonds.

(39) Yanson, I. K.; Teplitsky, A. B.; Sukhodub, L. F. *Biopolymers* **1979**, *18*, 1149.
(40) Santamaría, R.; Vázquez, A. *J. Comput. Chem.* **1994**, *9*, 981.
(41) Frey, P. A.; Whitt, S. A.; Tobin, J. B. *Science* **1994**, *264*, 1927.
(42) Pan, Y.; McAllister, M. A. *J. Org. Chem.* **1997**, *62*, 8171.
(43) Hush, N. S.; Cheung, A. S. *Chem. Phys. Lett.* **1975**, *34*, 11.

Scheme 2

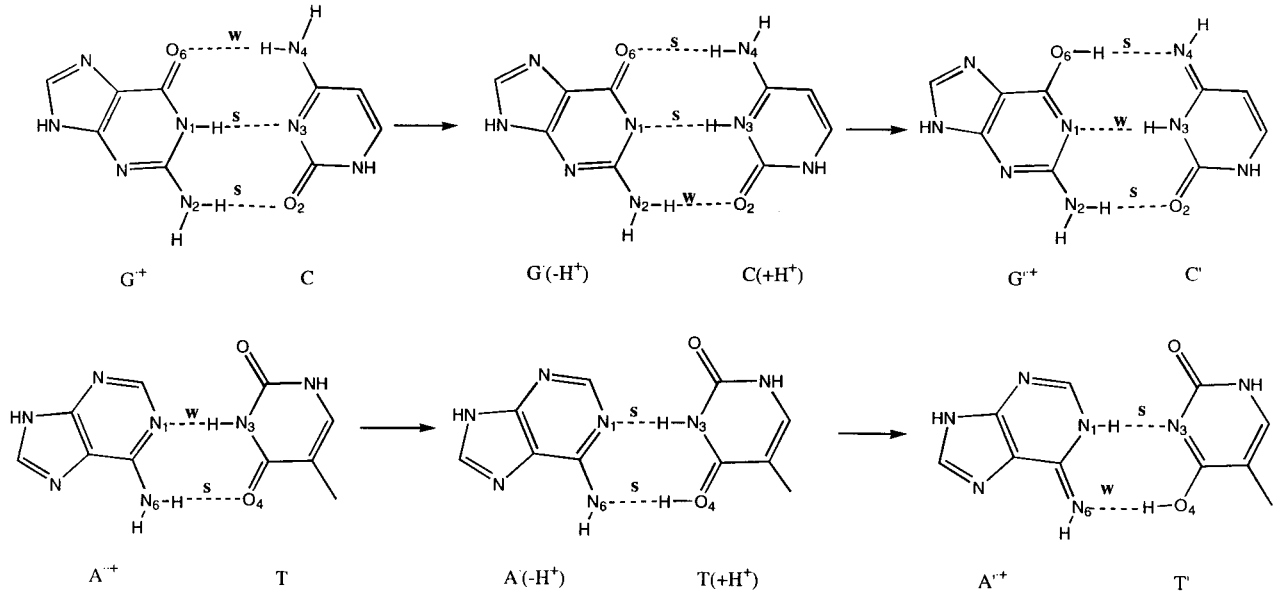

Table 4. B3LYP Relative Energies of GC and AT Radical Cations with Respect to Its Own Ground State Asymptote[c]

	(Guanine−Cytosine)$^{\bullet+}$				
	G$^{\bullet+}$ + C	G$^{\bullet+}$−C	G$^{\bullet}$(−H^{+})−C(+H^{+})	G$^{\bullet}$(−H^{+}) + C(+H^{+})	G′$^{\bullet+}$ + C′
ΔE	0.0	−48.4(−44.3)	−47.2(−43.2)	1.1	2.6
ΔE_0[a]	0.0	−46.8(−42.7)	−45.4(−41.4)	1.1	3.4
ΔH^0_f(298 K)[b]	0.0	−47.1(−43.0)	−45.7(−41.7)	1.3	3.1
ΔG^0_f(298 K)	0.0	−34.1(−30.0)	−32.7(−28.7)	0.6	3.7
	Adenine−Thymine				
	A$^{\bullet+}$ + T	A$^{\bullet+}$−T	A$^{\bullet}$(−H^{+})−T(+H^{+})	A′$^{\bullet+}$−T′	A$^{\bullet}$(−H^{+}) + T(+H^{+})	A′$^{\bullet+}$ + T′
ΔE	0.0	−25.4(−22.3)	−24.2(−21.2)	−18.9(−15.5)	24.7	17.5
ΔE_0[a]	0.0	−25.1(−22.0)	−24.3(−21.3)	−19.8(−16.4)	23.9	17.2
ΔH^0_f(298 K)[b]	0.0	−24.8(−21.7)	−24.3(−21.3)	−19.7(−16.3)	23.9	17.0
ΔG^0_f(298 K)	0.0	−13.6(−10.5)	−12.1(−9.1)	−7.7(−4.3)	24.1	17.4

[a] Includes zero point energy computed from the unscaled harmonic B3LYP frequencies. [b] After correction for translational, rotational, and vibrational energies determined at the B3LYP level. [c] In kcal/mol.

Figure 2b−c,e−g also show that, in addition to the variations of H-bond distances during the proton-transfer reactions, important geometry changes take also place in the rings of the purine and pirimidine monomers. This indicates that the studied processes have a high multidimensional character.

We have previously seen that Mulliken spin densities and charges indicate that ionization of GC and AT is mainly localized at the guanine and adenine monomers, respectively. For the G$^{\bullet}$(−H^{+})−C(+H^{+}) and A$^{\bullet}$(−H^{+})−T(+H^{+}) systems, the Mulliken charges of the C(+H^{+}) and T(+H^{+}) fragments are 0.82 and 0.76, respectively, which confirms that the nature of the G$^{\bullet+}$C → G$^{\bullet}$(−H^{+})−C(+H^{+}) and A$^{\bullet+}$T → A$^{\bullet}$(−H^{+})−T(+H^{+}) processes is that of a proton-transfer reaction. Consequently, the radical remains at the deprotonated Guanine and Adenine monomers, both of them showing a spin density value of 1.0. Therefore, the G$^{\bullet}$(−H^{+})−C(+H^{+}) and A$^{\bullet}$(−H^{+})−T(+H^{+}) systems are distonic radical cations,[44] since the net charge and the unpaired electron are localized in different fragments of the complex. For the A′$^{\bullet+}$−T′ system, the charge and spin density of adenine are 0.84 and 1.00, respectively. Charge and spin density are now in the same monomer as a consequence of the second proton-transfer reaction.

The relative energies of the different cationic species with respect to the ground-state asymptote are given in Table 4. For comparison we have included the relative energies of the single and double proton transferred asymptotes. Both for GC and AT radical cations, the global minima of the potential energy surface are the nonproton transferred G$^{\bullet+}$−C and A$^{\bullet+}$−T structures, respectively. The single proton transferred complexes, G$^{\bullet}$(−H^{+})−C(+H^{+}) and A$^{\bullet}$(−H^{+})−T(+H^{+}), however, are only 1.2 kcal/mol above the absolute minimum. Correcting for basis set superposition error decreases slightly the difference to 1.1 kcal/mol, while the inclusion of the zero point correction leads to a 1.4 and 0.8 kcal/mol energy differences for G$^{\bullet+}$−C and A$^{\bullet+}$−T, respectively. The minimum corresponding to the double proton-transferred A′$^{\bullet+}$−T′ complex, before and after correcting for BSSE, is 6.5 and 6.8 kcal/mol, respectively, higher than the initially ionized A$^{\bullet+}$−T structure. Inclusion of the zero point energy slightly decreases the energy difference to 5.3 kcal/mol. From the variation of the counterpoise corrected free energy at 298 K, the computed equilibrium constants for the single proton-transfer process in GC and AT are 0.11 and 0.09, respectively. For the double proton-transfer process in the AT cation, the equilibrium constant is 2.7×10^{-5}.

The stability of the different radical cations can be understood considering two factors: the stability of the asymptotes from which they derive and the strength of the interaction leading to the formation of the dimer. For GC radical cation, the nonproton transferred and the single proton-transferred asymptotes are almost degenerate; that is, the G$^{\bullet}$(−H^{+}) parent radical

(44) Yates, B. F.; Bouma, W.; Radom, L. *J. Am. Chem. Soc.* **1984**, *106*, 5805.

and Cytosine have very similar proton affinities. In particular, the $G^{\bullet}(-H^+) + C(+H^+)$ asymptote is 1.1 kcal/mol less stable than the $G^{\bullet+} + C$ one. As it can be observed, this difference is the same than that found between the $G^{\bullet}(-H^+)-C(+H^+)$ and the $G^{\bullet+}-C$ minima, which implies that the H-bond interaction is the same in the two structures. This is not surprising considering that the two minima show a similar (w−s−s) and (s−s−w) pattern with two neighbor strong H-bonds.

Table 4 show that the double proton-transferred asymptote, $G'^{\bullet+} + C'$, is also slightly less stable (2.6 kcal/mol) than the ground-state one. However, the interaction arising from this asymptote has a (s−w−s) pattern which, as it has been previously mentioned, is very unfavorable due to the presence of a central weak H-bond interaction. This is the main reason this minima does not appear on the potential energy surface.

For the AT cationic system, the single proton transferred asymptote lies much higher in energy (24.7 kcal/mol) than the ground-state one. However, the derived proton-transferred $A^{\bullet}(-H^+)-T(+H^+)$ dimer is almost degenerate with the non-proton transferred $A^{\bullet+}-T$ one. This is due to the fact that in $A^{\bullet+}-T$ we have one weak H-bond and one strong H-bond (w−s), while in $A^{\bullet}(-H^+)-T(+H^+)$ the two H-bonds are strong (s−s). It is also worth noting that the dissociation energy of $A^{\bullet}(-H^+)-T(+H^+)$ with respect to its own asymptote is 48.9 kcal/mol, very similar to that found in the GC radical cation where we also have two strong H-bonds. Thus, the new strong H-bond compensates for the destabilization of the proton transferred asymptote. For the model system formamidine−formamide, the proton-transferred asymptote does not lie as high in energy compared to the ground state (see Table 1). Thus, the derived dimer becomes more stable and, consequently, the only minimum on the potential energy surface.

As for the initial $A^{\bullet+}-T$ species, the double proton-transferred $A'^{\bullet+}-T'$ dimer has one strong H-bond and one weak H-bond. However, it lies only 6.5 kcal/mol above, despite having its asymptote 17.5 kcal/mol above the ground-state one. In this case, the difference is due to the fact that in the initial radical cation we have a N6−H···O4 strong bond, while in the double proton-transferred one we have a much stronger N1−H···N3 bond. As mentioned, the N1−N3 bond distance is much shorter than the sum of van der Waals radii.

Recent studies relate short strong hydrogen bonds with low-barrier hydrogen bonds.[38,41,42,45] The cationic systems studied in the present work present short-strong hydrogen bonds, and thus, it is interesting to study the proton transfer energy profiles connecting the obtained minima. Figure 3 shows the energy profile of the single and double proton transfer reactions in GC and AT radical cations. These energy profiles have been obtained optimizing the whole system for different fix values of a distinguished coordinate. Given that the distinguished coordinate does not differ significantly from the reaction coordinate and the chosen step is small enough, we expect the obtained maximum to lie only slightly higher than the real transition state. For GC, we have chosen the H−N3 distance as the distinguished coordinate in the single proton-transfer process. For the transfer of the second proton, we have chosen the O6−H distance. It can be observed in Figure 3a that the maximum of the energy profile of the first proton transfer is

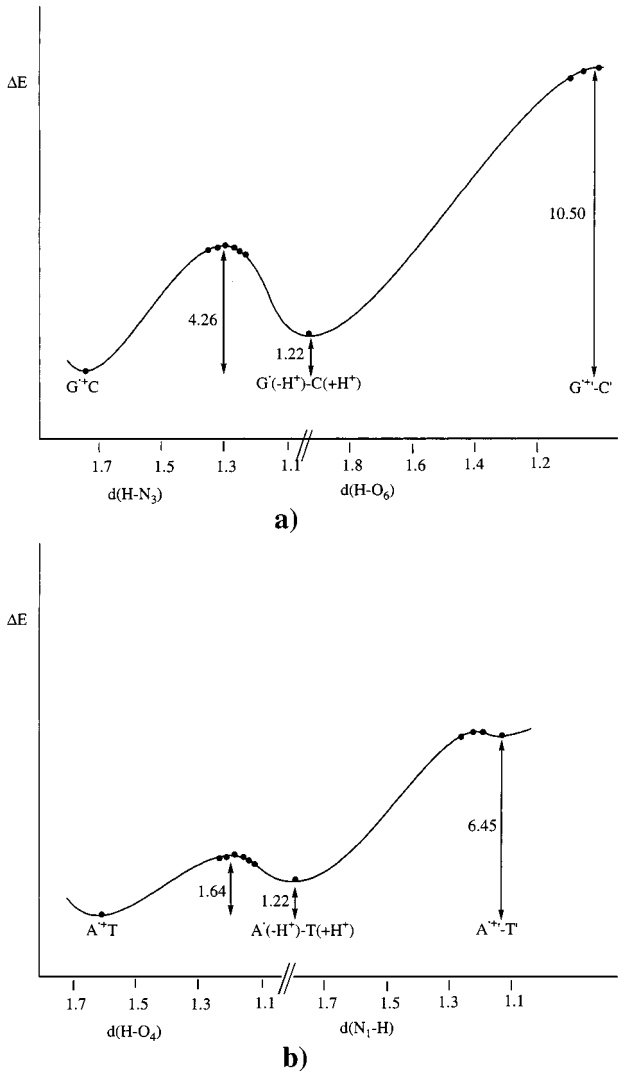

Figure 3. Enegery profiles for the single and double proton-transfer processes in cationic Guanine−Cytosine (a) and Adenine−Thymine (b) Watson Crick base pairs.

4.26 kcal/mol above the reactant. A similar value has been obtained using B3LYP energies at the UHF geometries.[9] The energy barrier for the reverse process is, thus, 3.04 kcal/mol. At this point ($d_{H-N3} = 1.30$ Å), the distance between the two heavy atoms is 2.63 Å, about 0.2 Å smaller than in $G^{\bullet+}-C$. This shortening of the distance between the two heavy atoms is typical in this kind of processes. Although the energy barrier is low, it does not fall within the category of low-barrier hydrogen bond. For the double proton-transfer process, the energy increases monotonically with the shortening of the O6−H distance. At a value of 1.05 Å for the O6−H distance, which could be taken as the double proton transferred structure, the energy is about 10 kcal/mol higher than the $G^{+\bullet}-C$ global minimum. Thus, it is not surprising that all the attempts to optimize such structure lead to the $G^{\bullet}(-H^+)-C(+H^+)$ complex.

For the AT radical cation, the distinguished coordinates used for the single and double proton-transfer reactions are the H−O4 and the N1−H distances, respectively. For this system, the single proton-transfer reaction shows a smaller energy barrier (1.64 kcal/mol) compared to the GC radical cation. The reverse reaction has an energy barrier of only 0.42 kcal/mol. At the maximum of the energy profile the distinguished coordinate has a value of 1.20 Å. As for GC, at this point the distance between the two heavy atoms decreases about 0.2 Å when compared to

(45) (a) Cleland, W. W. *Biochemistry* **1992**, *31*, 317. (b) Cleland, W. W.; Kreevoy, M. M. *Science* **1994**, *264*, 1887. (c) García-Viloca, M.; González-Lafont, A.; Lluch, J. M. *J. Phys. Chem. A* **1997**, *101*, 3880. (d) García-Viloca, M.; González-Lafont, A, Lluch, J. M. *J. Am. Chem. Soc.* **1997**, *119*, 1081. (e) Pan, Y.; McAllister, M. A. *J. Am. Chem. Soc.* **1997**, *119*, 7561. (f) Gilli, P.; Bertolasi, V.; Ferreti, V.; Gilli, G. *J. Am. Chem. Soc.* **1994**, *116*, 909. (g) Hibbert, F.; Emsley, J. *Adv. Phys. Org. Chem.* **1990**, *26*, 255.

the reactants. However, since the H-bond distances in AT are shorter than in GC (see Figure 2), it is not surprising that we get a lower energy barrier for AT. Therefore, the AT system behaves more as a strong short low-barrier hydrogen bond than GC. The energy profile for the double proton-transfer reaction shows a very shallow minima. The computed harmonic frequency calculations for this structure show that the vibrational frequency corresponding to the H transfer is 39 cm^{-1} which is consistent with a very close transition state and with a small energy barrier. This frequency value is much smaller than that obtained for the A$^{\bullet}(-H^{+})-T(+H^{+})$ structure (370 cm^{-1}) for which the energy barrier of the proton transfer is 0.42 kcal/mol. Thus, although this frequency is a local property, it can be correlated with the height of the barrier. The energy barrier for the second proton transfer is slightly larger than the reaction energy (6.45 kcal/mol). The reverse reaction has almost no barrier in agreement with a very short strong H-bond.

5. Concluding Remarks

Single proton-transfer reactions for Watson−Crick GC and AT radical cations are favorable processes both from a thermodynamic and a kinetic point of view. Although the double proton species do not lie high in energy compared to the reactant, they are not expected to be detected in the experiments, given that the barrier of conversion to the single proton transferred structures is negligible. The difference between the vertical and adiabatic ionization potentials provides the excess of vibrational energy present after ionization. In both systems, GC and AT, this excess is higher than the energy barrier of the single proton transfer reaction. Therefore, if an important amount of this excess is redistributed in the vibrational modes involved in the proton transfer process, the proton would not be localized in any of the two structures. Even if the excess of vibrational energy is not conveniently redistributed, we could also have a delocalization of the proton produced by tunnel effect. That is, the energy profile of the proton transfer process depends on the position of the heavy atoms. For instance, for GC the nonproton transferred structure is destabilized by 8.3 kcal/mol if the geometry of the heavy atoms is that of the proton-transfer structure. Therefore, some of the geometry fluctuations of the heavy atoms can change the energy profile to a symmetrical double well situation where tunneling can occur readily. A similar situation has been discussed previously when dealing with solvent fluctuations.[46]

The behavior of the radical cation species is very different to that observed for the neutral base pairs, where the single proton-transfer reaction was found to be very unfavorable due to the formation of an ion−pair complex. The double proton-transfer reaction was found to be concerted or two-step depending on the level of calculation but always with a high barrier.[13c] In any case, the double proton-transfer structure was computed to be more stable than the single proton transfer one. The situation does not change dramatically at the excited states.[47] On the contrary, for the radical cations the single proton transfer is a very favorable process due to the increased acidity of the ionized monomer[48] and to the fact that the proton transfer does not imply a creation of charges but a transfer of a positive charge. Thus, the two-step mechanism is the preferred one in the double proton-transfer process in radical cations.

When the system has two or more hydrogen bonds, the energy profile is not only determined by the proton affinity of the centers involved in the proton transfer[15] but also by the number and sequence of the strong and weak hydrogen bonds formed. That is, for the same number of strong short hydrogen bonds, the most stable situations are those in which the strong hydrogen bonds are neighbors, the alternate situations being much more unstable. According to these arguments and considering that in the ground state the ionized monomer in the dimer is that with the lowest ionization potential (guanine and adenine, respectively) we can generalize the present results, obtained for the Watson−Crick pairs, to other possible gas-phase pairings. For instance, for the reverse Watson−Crick AT, Hoogsteen AT, and reverse Hoogsten AT, we expect a similar energy profile than the one found here for the Watson−Crick AT, since the initial ionized dimer will have one weak H-bond and one strong H-bond, that will become two strong H-bonds after the proton transfer occurs. Certainly, the relative stability of the two minima will also depend on the stability of the asymptotes from which they derive. On the contrary, for the reverse GC, we expect the initial ionized system (s−s) to be significantly more stable than the single proton-transferred one (w−s). For Hoogsten GC^{+} and reverse Hoogsteen GC^{+}, Guanine acts as proton acceptor, and so, its ionization will weaken the two H-bond interactions. The dimer would probably dissociate considering the repulsive electrostatic interaction between the two positive charges. Therefore, the single proton transfer reaction in the GC radical cation is only expected to be produced in the Watson−Crick pairing.

In the different proton-transfer processes that have been described for GC and AT radical cations, Guanine and Adenine are always the fragments that show the radical character. The neutral G$^{\bullet}(-H^{+})$ and A$^{\bullet}(-H^{+})$ radicals formed after the single proton-transfer reaction have been invoked to play an important role in the DNA damage caused by ionization.[1e] New gas-phase experiments on these systems would be desirable in order to test the present theoretical predictions and obtain the fruitful sinergy between theory and experiment for advancing the knowledge of chemical and biochemical processes.

JA9804417

(46) (a) Staib, A.; Borgis, D.; Hynes, J. T. *J. Chem. Phys.* **1995**, *102*, 2487. (b) Borgis, D.; Hynes, J. T. *J. Phys. Chem.* **1996**, *100*, 1118. (c) Cukier, R. I.; Zhu, J. *J. Phys. Chem.* **1997**, *101*, 7180.

(47) Guallar, V.; Douhal, A.; Moreno, M.; Lluch, J. M. personal communication.

(48) (a) Gill, P. M. W.; Radom, L. *J. Am. Chem. Soc.* **1988**, *100*, 4931. (b) Sodupe, M.; Oliva, A.; Bertran, J. *J. Am. Chem. Soc.* **1994**, *116*, 8249. (c) Sodupe, M.; Oliva, A.; Bertran, J. *J. Am. Chem. Soc.* **1995**, *117*, 8416.